Multiangle Backscattering Observations of Continental Surfaces in Ku-Band (13 GHz) From Satellites: Understanding the Signals, Particularly in Arid Regions

Catherine Prigent, Filipe Aires, Carlos Jimenez, Fabrice Papa, and Jack Roger

***Abstract*—Backscattering in Ku-band (13 GHz) over continental surfaces is analyzed, with the Tropical Rainfall Measurement Mission/Precipitation Radar instruments (incidence angles from 0° to 18°), along with observations from the Topex–Poseidon nadir-looking altimeter and the QuikSCAT scatterometer (incidence angles around 50°). The signals from the three instruments are very consistent. The backscattering tends to decrease with increasing vegetation density, as expected, making it possible to classify vegetation density with active microwaves. Over the northern African desert, a very large spatial variability of the backscattering is observed, with both surface and volume scatterings contributing to the signals. The use of multiangle observations does help characterizing the desert types, but in some areas, the ambiguity of the signals is still unexplained. The French–Chinese joint mission "Chinese–French Oceanic SATellite" will carry two active microwave instruments with a large range of incidence angles, from 0° to 50°. We show that the combined use of observations at low and high incidence angles adds information, particularly over desert surfaces.**

***Index Terms*—Altimetry, radar remote sensing, surface roughness.**

I. Introduction

BACKSCATTERING over continental surfaces at large incidence angles from scatterometers is commonly used for land surface characterization. Global soil moisture estimations are derived from observations at 5 GHz with the European Remote Sensing Satellite scatterometer, with ASCAT on board MetOp (e.g., [1] and [2]) or from QuikSCAT observations at 13 GHz (e.g., [3]). The sensitivity of these observations to the vegetation has also triggered some analysis (e.g., [4]–[7]), and the complementarity to the classic visible/near-infrared Normalized Vegetation Index has been shown [8]. Arid and semiarid regions have also been studied with backscattering observations, with the estimation of the aerodynamic roughness lengths for the modeling of aerosol emission [9], [10].

At lower incidence angles, the Precipitation Radar (PR) on board the Tropical Rainfall Measurement Mission (TRMM) observes the Earth at 13 GHz, from nadir to 18°, to estimate precipitation. Under rain-free condition, it also observes the surfaces, but so far, analysis of the PR measurements for surface studies has been rather limited [11] and essentially directed toward the improvement of the precipitation retrieval [12], [13]. At nadir, altimetric missions such as Topex–Poseidon (TP) have also provided backscattering information over continents, with some interests for surface characterizations, in addition to their use for inland waters [14]–[16].

Over the ocean, backscattering models have been developed to describe the interaction between the surface and the radar signal. Over land, the interaction is more complicated, with a larger spatial heterogeneity, and the complex presence of soil, vegetation, and possibly snow. Both surface and volume scatterings can be at play, and modeling simultaneously these two effects is very difficult.

The Chinese [China National Space Administration (CNSA)] and French [Centre National d'Etudes Spatiales (CNES)] space agencies will launch the Chinese–French Oceanic SATellite (CFOSAT) mission in 2014, with two microwave active instruments on board, at Ku-band (13.2–13.6 GHz). The wave-scatterometer spectrometer, Surface Waves Investigation and Monitoring (SWIM), is a six-beam radar at small incidences (0° to 10°) supplied by CNES. The scatterometer (SCAT) is a rotating fan-beam radar with larger incidence angles (from 18° to 50°) supplied by CNSA. This combination of incidence angles will make it possible to measure both wind vector (from large incidence) and wave properties (from small incidence). The primary objective of CFOSAT is to monitor the wind and waves at the ocean surface in order to improve the forecast for marine meteorology and our understanding of the ocean surface processes. However, it will also collect information over the continents, and a secondary objective is to characterize

Manuscript received January 21, 2014; revised May 7, 2014; accepted June 23, 2014. This work was supported in part by the Centre National d'Etudes Spatiales TOSCA program related to the Chinese–French Oceanic SATellite preparation.

C. Prigent is with the Laboratoire d'Etudes du Rayonnement et de la Matière en Astrophysique, Observatoire de Paris, 75014 Paris, France.

F. Aires and C. Jimenez are with Estellus, 75002 Paris, France, and also with the Laboratoire d'Etudes du Rayonnement et de la Matière en Astrophysique, Observatoire de Paris, 75014 Paris, France.

F. Papa is with the Laboratoire d'Etudes en Géophysique et Océanographie Spatiales, Institut de Recherche pour le Développement (IRD), 34104 Toulouse, France, and also with the Indo–French Cell for Water Sciences, IRD–Indian Institute of Science (IISc) Joint International Laboratory, IISc, Bangalore 560012, India.

J. Roger, retired, was with the Bureau de Recherche Géologique et Minière, 45100 Orléans, France.

Color versions of one or more of the figures in this paper are available online at http://ieeexplore.ieee.org.

Digital Object Identifier 10.1109/TGRS.2014.2338913

land surfaces, particularly arid regions for better modeling and forecast of emission of mineral dust.

In the framework of the preparation for the CFOSAT mission, the objective of this study is to analyze the available backscattering measurements of continental surfaces in Ku-band (13 GHz), under a large range of incidence angles. This will help better understand the prevailing interactions between the surface and the radiation, for a possible use of the combined SWIM and SCAT observations to characterize the land surfaces, particularly in arid regions.

Existing Ku (13 GHz) backscattering observations of continental surfaces are gathered (Section II): the PR observations on board TRMM [as processed at the National Aeronautics and Space Administration (NASA)] covering incidence angles from 0° to 18°, QuikSCAT measurements at 46° and 54° incidence angles, and the TP altimeter (0°). All data are available over a full annual cycle, on a monthly average basis, in the $\pm 36.25°$ region covered by TRMM. The data are analyzed over the full area, first insisting on the variation of the backscattering with vegetation and incidence angles, over the year (Section III). Then, the study focuses in the arid and semiarid regions in North Africa and the Arabian Peninsula, where the spatial variability is larger regardless of the observing incidence angle (Section III), with the objective of documenting the complex interactions between the surface and the radar signals. Section IV concludes this paper.

II. Available Satellite Surface Backscattering in Ku-Band

A. TRMM PR

TRMM, a joint mission between NASA and the Japan Aerospace Exploration Agency, is primarily designed to monitor and study tropical rainfall [17]. TRMM platform is on a low equatorial orbit, and it observes the intertropical zone ($\pm 40°$). It includes an active microwave instrument, the PR, an electronically scanning radar operating at 13.8 GHz in horizontal polarization for both transmission and reception (HH polarization). The PR was the first spaceborne instrument designed to provide 3-D maps of rain structure, over both land and ocean. It observes the Earth in a cross-track mode, with incidence angles up to 18° on both sides of the nadir view to cover a swath of 250 km. It has horizontal resolution at the ground of 5 km at nadir. Under rain-free conditions, the backscattering signal corresponds to the Earth surface response. Given the scanning geometry of the PR, each location is not observed often under the same incidence angle. In order to analyze the variability of the land surface backscattering with locations and incidence angles, the normalized radar backscattering cross sections have been collected at NASA and stored with a 0.1° spatial sampling in latitude and longitude, for 26 incidence angle ranges from 0° to 18°, with a 0.75° increment. The azimuth angle is not taken into account and the left- and right-hand sides of the scan are not separated. The data are averaged from 1998 to 2009, for each month (one month will represent the 12-year average). This time averaging is necessary to have enough observations of a given location and incidence angle, at 0.1° spatial resolution.

B. QuikSCAT Scatterometer and the TP Altimeter

For comparison purposes, we will also analyze the observations from two other instruments operating in Ku-band, the QuikSCAT scatterometer and the TP altimeter.

The NASA QuikSCAT mission, launched in 1999, includes a scatterometer (SeaWinds) observing at 13.4 GHz. The instrument uses a rotating dish antenna with two spot beams that conically sweep, with incidence angles of 46° (HH polarization) and 54° (VV polarization). The antenna has a 7 km × 25 km field of view, and the swath is 1800 km wide. It provides approximately 90% coverage of the Earth every day. The SeaWinds instrument is described in [18]. Its first objective is the estimation of the wind speed and direction over ocean, but a few studies analyzed the possibility to characterize land properties with these observations, particularly soil moisture and vegetation (e.g., [3] and [19]–[21]). For analysis purposes, the observations are projected on a grid and monthly averaged, for each incidence angle, regardless of the azimuth angle.

TP is a joint U.S.–French radar altimeter mission initially developed to make accurate measurements of sea level [22]. Launched in 1992, TP observes the ocean and continental surfaces at nadir (0°) along its orbit ground track with a ten-day repeat cycle. Its equatorial ground spacing is about 300 km, and its swath width only amounts to a few kilometers (∼5 km), meaning that the global coverage is limited. In this paper, observations are from the main instrument, the NASA Radar Altimeter, operating in Ku-band (13.6 GHz) and C-band (5.4 GHz).

In this paper, we use the backscattering coefficient measurements from TP, expressed in decibels, that are coming originally from the Aviso database (merged TP Geophysical Data Records [23]), now also accessible at the Centre de Topographie des Océans et de l'Hydrosphère (http://ctoh.legos.obs-mip.fr/).

Observations from QuikSCAT and TP instruments are collected for 2000 and monthly averaged, on the same horizontal grid (equal-area grid of $0.25° \times 0.25°$ at the equator). Note that there is not a full temporal coincidence with the PR data that is averaged over 12 years. First, the comparison is used to confirm the spatial structures observed with the PR at 0°. Second, the comparisons will be essentially analyzed for the arid regions where limited interannual variability is expected.

Table I summarizes the characteristics of the instruments used in this study.

III. Global Analysis

Fig. 1 represents the PR backscattering at 0° and 18°, for January and July, averaged over 1998–2009 (the color scales have the same amplitude but not the same values). In general, the backscattering tends to increase with decreasing vegetation density at 0°, whereas it decreases at 18°. In the absence of vegetation, scattering at the soil interface is essentially related to surface scattering, although volume scattering can occur under dry conditions when the radiation can penetrate the subsurface. The scattering at the soil interface is driven by the soil moisture and roughness. Over a smooth surface, specular reflexion will lead to strong backscattering at nadir but very limited return at larger incidence angles. This is often observed

TABLE I
SUMMARY OF THE INSTRUMENT CHARACTERISTICS AND CORRESPONDING PROCESSING GRID

Mission	Instrument	Frequency	Polarization	Incidence angle	Spatial resolution	Processing grid
TRMM	PR	13.8 GHz	HH	0° to 18°	5 km	0.1°x 0.1°
QuikSCAT	SeaWinds	13.4 GHz	HH	46°	25 km	0.25°x 0.25°
			VV	54°	5 km	
Topex-Poseidon	NRA	13.6 GHz		0 °	5 km	0.25°x 0.25°

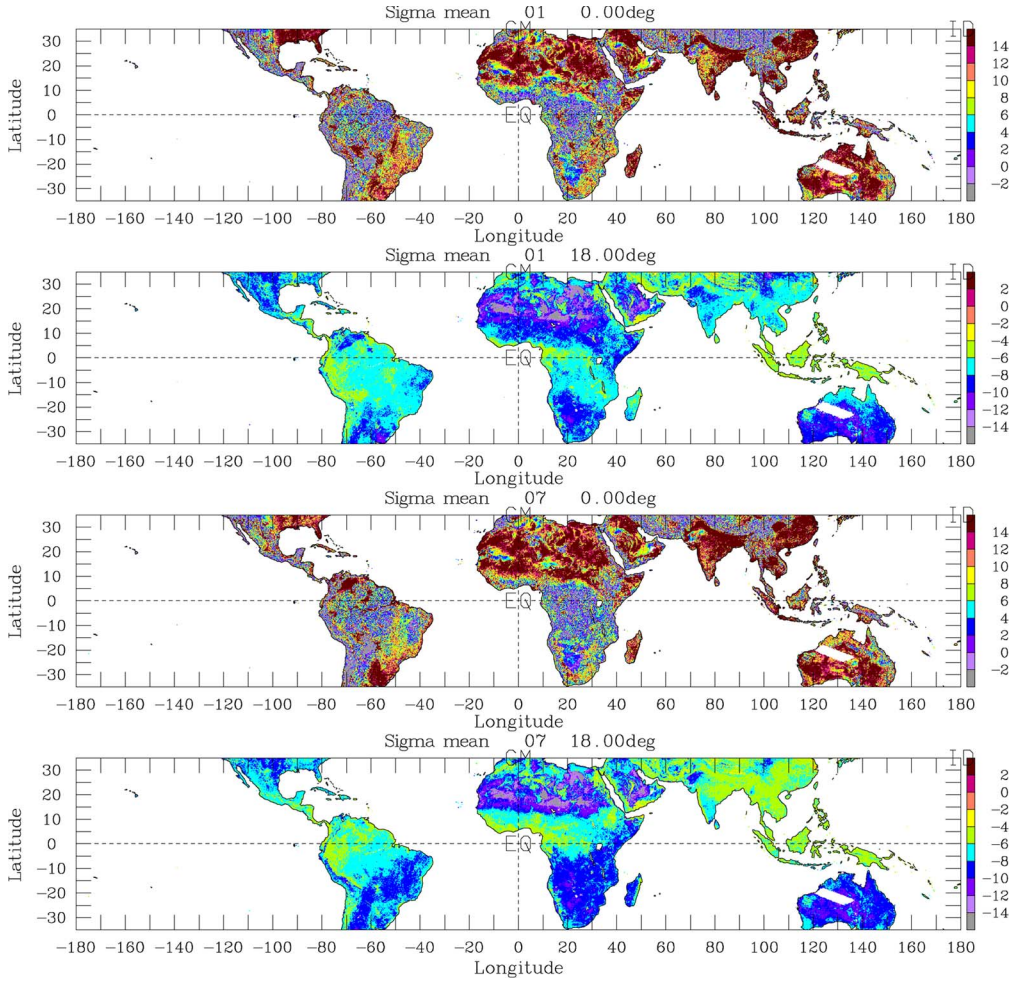

Fig. 1. PR backscattering (in decibels) at 0° and 18° for (two top figures) January and (two bottom figures) July.

in deserts, as can be seen in Fig. 1 in North Africa, or in standing water regions like in northern India. Scattering in vegetation corresponds to volume scattering. At nadir, scattering over dense vegetation will induce a weaker radar return than over most deserts, contrarily to what happens at larger incidence angles (see the responses of the equatorial forest in Africa or Brazil). The response at 0° shows more spatial variability than at 18°. It also presents more temporal variability at monthly time scale (not shown). This is only partly due to the mean number of observations per pixel being twice smaller at 0° than at the other angles, because of the symmetry of the scan around nadir. There are averages of ∼18 observations per pixel at nadir and ∼36 for the other angles, at 0.1° spatial resolution, for each month. These numbers are rather low despite the 12-year average (this actually justifies the 12-year average). The mean temporal variance values (averaged over space and time) are ∼4.5 dB at nadir and ∼1.1 dB for large angles. Note nevertheless that, despite similar numbers of observations for all angles except nadir, there is a small smooth decrease of the temporal variance with angles between 0.75° (∼2.8 dB) and the large angles (∼1.1 dB), related to the larger variability of the surface responses for low incidence angles. In Fig. 1, the seasonal changes between January and July appear clearer at 18° than at nadir. The scattering in the transition zone between the North African desert and the equatorial forest increases from January to July, related to the vegetation increase. No significant change is observable at nadir, partly due to the larger noise. However, an increase in the backscattering can be observed at nadir with

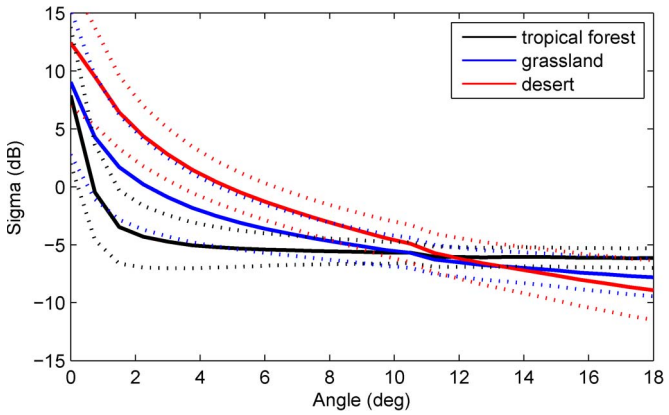

Fig. 2. PR backscattering as a function of angle, for different vegetation types, for PR TRMM, for July, for the vegetation classification of Matthews (1983). For each vegetation type, one standard deviation is indicated with the dotted lines.

the presence of standing water. The backscattering at 0° is much larger in South America in the Orinoco Basin or around the Parana in July when the wetlands are inundated than in January. This is not clearly observed at 18°. That was already mentioned and studied at larger incidence angles [8].

Azimuthal variations of the signal have been observed over land, over different surface types such as desert (e.g., [24] and [25]) or ice sheet [26]. Regions with predominant surface slopes at large scale (on the order of the satellite field of view), such as mountainous regions or ice sheets, can generate azimuthal asymmetry. In addition, for structures with predominant orientation and comparable in size with the wavelength, the backscattered signal can be subjected to constructive interference, through the resonant Bragg scattering. The authors in [25] analyzed and modeled the different mechanisms that can generate azimuthal asymmetry, in order to normalize the backscatter for use in soil moisture retrieval algorithms. The authors [24] carefully examined the backscatter signal from ergs (sand dunes) in the Sahara and concluded that the azimuthal information can help identify the dune direction and, as a consequence, the dominant wind direction. In this paper, the backscattering data have been systematically averaged over time regardless of the azimuth angle, limiting this modulation effect.

The different instruments emit and receive in the same polarizations (HH for TRMM, HH at 46°, and VV at 54° for QuikSCAT, TP observing at nadir; H and V are equivalent). Both surface and volume scatterings can depolarize the signal. Comparisons of 46° HH and 54° VV signals do not show obvious differences at the spatial scales of the QuikSCAT instrument.

The angular dependence of the backscattering coefficient is presented in Fig. 2, for different vegetation types. The vegetation classification from [27] is chosen here, along with the corresponding land use data set: It has been regrouped into ten classes [8]. Close to nadir, large angular dependences are observed for all surface types. For larger angles, the angular dependence decreases with increasing vegetation. There is a limited angle dependence for tropical forest, for angles larger than 3°, whereas for deserts, the backscattering coefficient strongly decreases with angles. The standard deviation is also indicated in Fig. 2, and it confirms that, at nadir, the variability of the backscattering decreases for larger incidence angles. Around

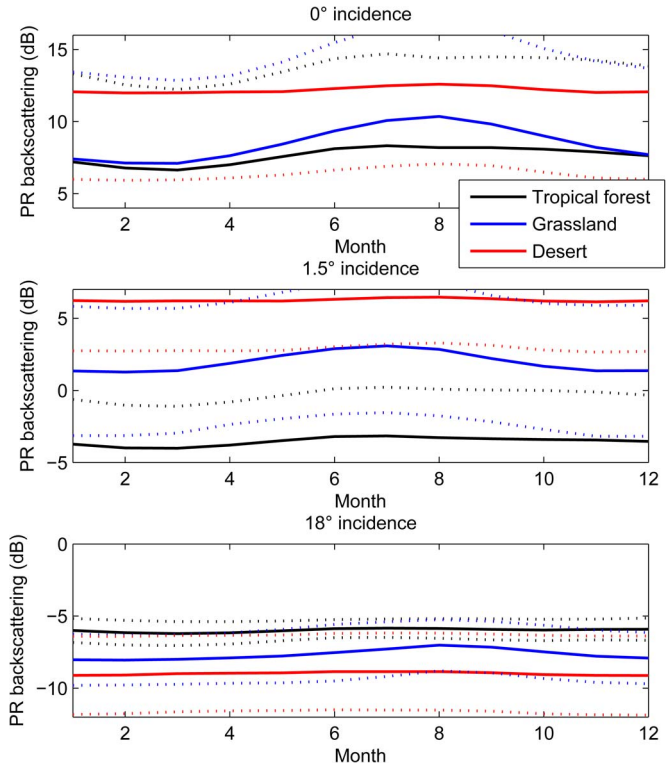

Fig. 3. PR backscattering (in decibels) as a function of the month, for three vegetation types and three incidence angles.

11°, all curves intersect. A small discontinuity is evidenced in the angular dependence also around 11°: It is explained by an instrument artifact in [13].

Fig. 3 shows the seasonal variation of the backscattering coefficients, for three surface types and three incidence angles, for the Northern Hemisphere between 0° and 40° N. As expected, the seasonal change is more pronounced for grassland. It appears larger for smaller angles but with a much larger variability (in the dashed line in Fig. 3) for small angles (not only in space but also in time).

An unsupervised classification has been applied to the TRMM backscattering observations (all 25 angles) to assess the potential of this type of measurement for vegetation classification. A preliminary exploration is provided here. A Kohonen classification [28] is adopted as it provides a neighboring requirement on the clusters, making their interpretation easier [8]. Fig. 4 shows the results for ten clusters, for July. The first clusters are representative of the arid regions, whereas the last ones characterize the dense vegetation. The spatial structure of the classification is consistent with the expectations, with the same class present in the regions where the same surface types are present. For instance, the transition zones from arid to dense vegetation are also well represented in Africa, from the north to the south. Some confusions in the classification appear between semiarid regions and likely wet areas such as the Orinoco Basin in Venezuela or the Bangal Delta in Bangladesh (class 3). Adding clusters to the classification would help solve these ambiguities. Fig. 5 presents the center of the clusters for each class, for different incidence angles. For each incidence angle, the evolution of the backscattering as a function of the

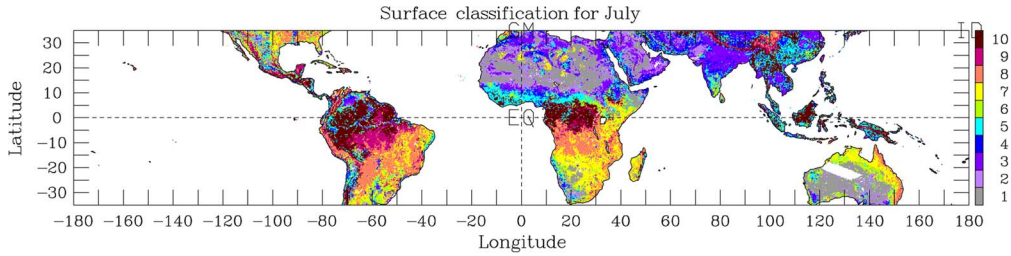

Fig. 4. Surface classification using all backscattering angles from PR for July.

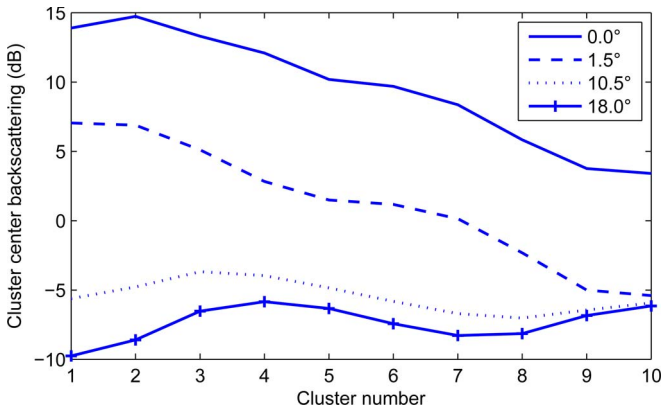

Fig. 5. Values of the PR backscattering (in decibels) for the centers for each cluster (see Fig. 4), for four incidence angles, as provided by the unsupervised classification.

cluster is different: The classification scheme benefits from the complementary information to define the clusters.

As a conclusion, the backscattering information at multiple angles can provide information on the surface types and can be exploited to classify the vegetation. This information can complement the analysis provided by other wavelength ranges, such as the Normalized Vegetation Index provided by visible and near-infrared observations [8].

IV. Analysis of Arid Surfaces

As seen in the previous section, a very large spatial variability of the backscattering coefficient is observed over arid regions for all incidence angles. Fig. 6 zooms on the backscattering signatures over North Africa and the Arabian Peninsula, for three TRMM/PR incidence angles (0°, 9.75°, and 18°), for July. TP (0° incidence angle) and QuikSCAT (54° incidence angle) responses are also presented, over the same area for the same month (Fig. 6). The TP altimeter has a limited coverage, as expected from its narrow and fixed swath. Regardless of the instrument and incidence angle, we verified that the observed spatial structures are rather stable with time, in the arid regions. However, they can vary in semiarid areas that can be subject to soil moisture or vegetation changes, such as the region south of 15° N.

To help the interpretation of the backscattering coefficients, Fig. 7 presents the topography in the region, as well as the map of the "sand dunes and shifting sand" of the Food and Agriculture Organization [29].

For large incidence angles (PR at 18° and QuikSCAT at 54°), the spatial structures are very similar with a spatial correlation coefficient of 0.85. For the two observation sources for large

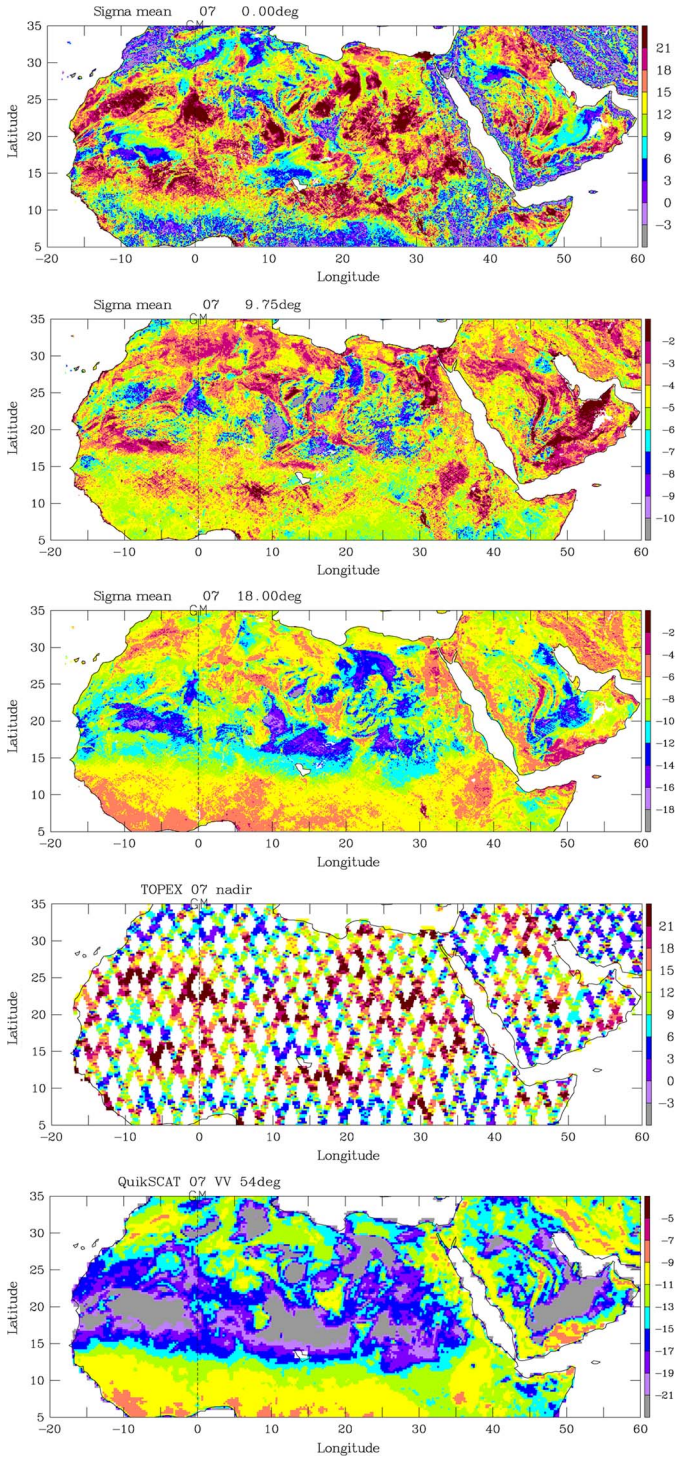

Fig. 6. (From top to bottom) Backscattering (in decibels) from PR at three incidence angles (0°, 9.75°, and 18°), along with (top) TP (0° incidence angle) and (bottom) QuikSCAT (54° incidence angle), over North Africa for July.

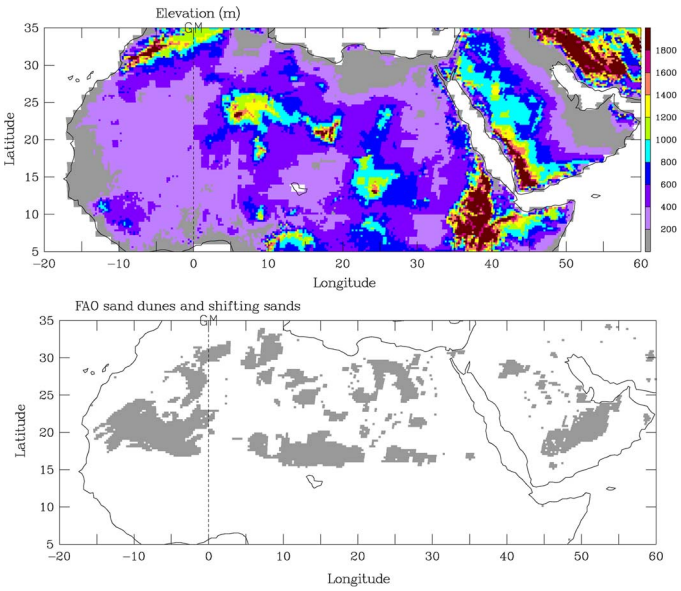

Fig. 7. Over North Africa, topography in (top) m and (bottom) FAO sand dunes and shifting sands.

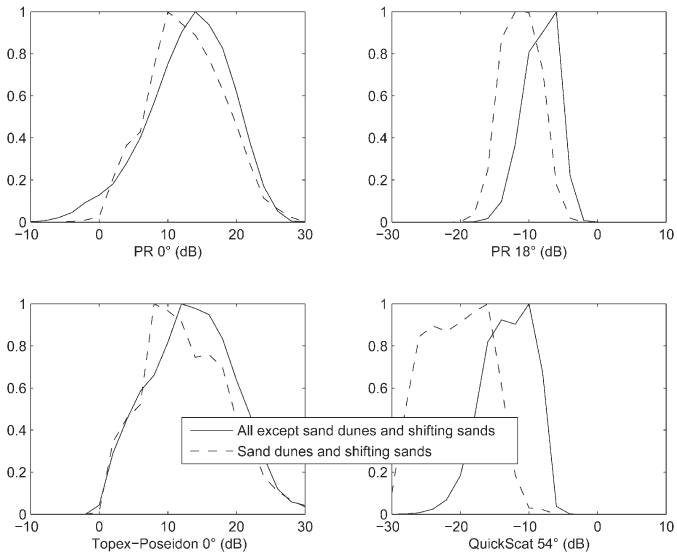

Fig. 8. Normalized histogram of the backscattering (in decibels) for the North African domain, for the PR at (top left) 0° and (top right) 18°, (bottom left) for TP at 0°, and (bottom right) for QuikSCAT at 54°, separately for the FAO "sand dunes and shifting sands" and for the rest of the region. Only pixels common to all instruments are considered.

incidence angles, the sand deserts (for instance, in Lybia or Saudi Arabia) are related to low-backscattering coefficients. The conjunction of two effects can contribute to these signatures. First, surface reflection on a flat desert surface observed with a significant angle of incidence will likely produce low backscattering. Second, volume scattering in a very dry medium such as dry sand can also yield low backscattering. The mountainous regions (the Atlas in Morocco, the Tibesti in Chad, or the Jabal al Hijaz in Saudi Arabia) correspond to higher backscattering coefficient, due to the large-scale roughness associated to the orography.

The spatial structures observed with the PR at 0° and with the TP altimeter (also at nadir) are very consistent, even in areas where a large spatial variability is observed. Note, for instance, the regions between 15° E and 0° and between 17° N and 22° N, where the PR and TP 0° backscatters change from 2 to 18 dB (the same for the sand desert south of Saudi Arabia). The spatial correlation coefficient between the two data sources is 0.67. This is rather low, but this is expected considering the large noise associated to the backscattering at 0°. At nadir, large backscatters are associated to flat surfaces, whereas smaller backscatters can be due to surface scattering (rough surfaces) or/and to volume scattering (dry surfaces). Sensitivity of the backscatter to soil moisture at nadir has also been evidenced in arid and semiarid regions [30]–[32].

The normalized histograms of the backscatters are presented for the North Africa and the Arabian Peninsula, separating the FAO "sand dunes and shifting sands" from the other surfaces, for PR at 0° and 18°, for TP at 0°, and for QuikSCAT at 54° (Fig. 8). Only the areas covered by all three instruments are considered so that statistics can be compared. At 0° incidence angle, for both PR and TP, the histograms for the sandy areas and for the rest of the region are rather broad and overlap significantly, despite the ∼5-dB difference in the maximum of the distribution. The lower backscattering for the sand dunes is likely related to volume scattering in the dry sand. For the larger incidence angles, the histograms of the two surface types are better separated; the larger the incidence angle, the larger the distance between the two histograms, as expected from the combined effect of more specularity and higher volume scattering in sand dunes.

Fig. 9 shows two transects in longitude over the North African desert, one at 10° W (top), the other one at 17.5° E (bottom). It clearly shows that the spatial structures observed at nadir with the PR and TP are very consistent. It also confirms the very good correspondence between the PR observations at 18° and the QuikSCAT observations. Note that the 46° and 54° observations show limited differences, despite the difference in polarizations (HH and VV, respectively) in addition to the difference in angle. The variations of the backscattering at 0°, although very consistent for the PR and TP, are difficult to interpret, except in the mountainous regions (e.g., the Tibesti around 22° N on the transect at 17.5° E) where the backscattering coefficients are all very similar, regardless of the incidence angle. In nonmountainous regions, the signal at 0° can show significant changes without any obvious variations in the other observations, nor with evident changes in the surface properties. The difference between the C-band (5 GHz) and Ku-band (13 GHz) for TP is also presented (middle panel). This difference is expected to be related to changes in penetration in the medium; the higher the differences, the larger the volume scattering [14]. However, no clear signals are observed here, likely due to the rather large noise of the backscattering at nadir.

The region north of the Tibesti, the Sarir Tibasti around 17.5° E and 25° N, is typical of high PR backscatter at 0° and low PR backscatter at 18° (see Figs. 6 and 9). Note that the region with the larger PR backscatter at 0° does not correspond to sand dunes or shifting sands, as described by the FAO (see Figs. 7 and 9). It is a very flat region where microwaves cannot penetrate. Its flatness yields high backscattering at 0° and low one for large incidence angles. Because of its hard surface, there

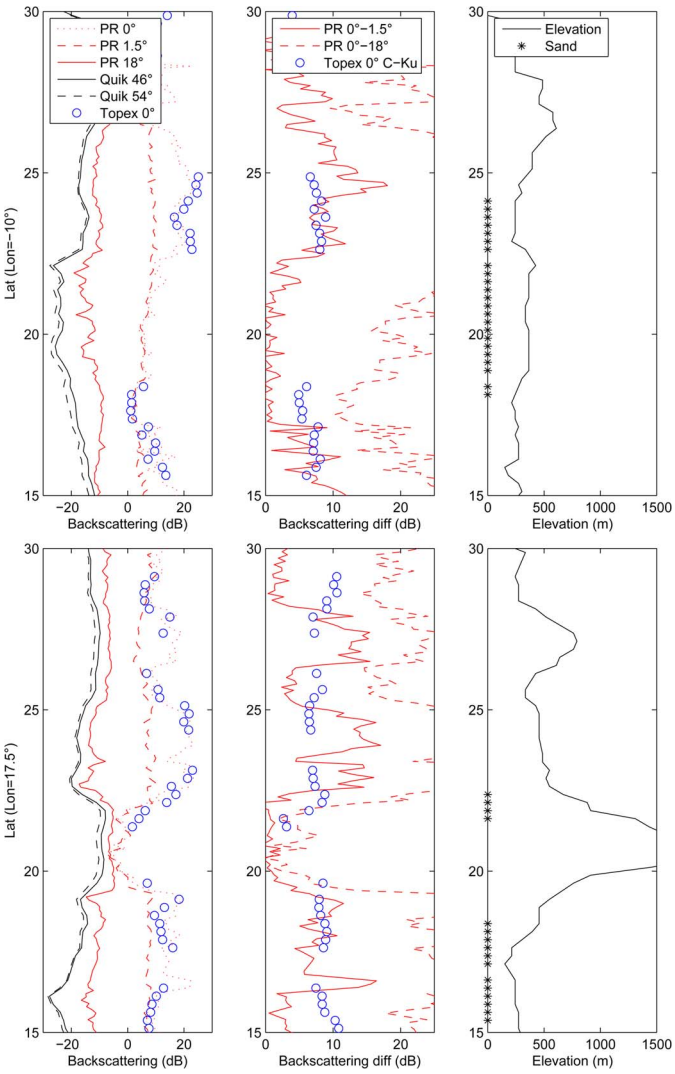

Fig. 9. Longitudinal transects in deserts at (top) 10° W and (bottom) 17.5° E. (Left) For the individual backscattering observations in Ku-band (13 GHz) from PR (at 0°, 1.5°, and 18°), QuikSCAT (at 46° and 54°), and Topex (at 0°). (Middle) For the difference between PR at 0° and PR at 1.5°, for the difference between PR at 0° and PR at 18°, and for the difference for Topex at 0° between C-band (5 GHz) and Ku-band (13 GHz). (Right) Location of the sand dunes and shifting sands (∗) and the elevation.

is limited volume scattering that could lower the backscattering, particularly observable at 0°.

On the contrary, the sandy deserts, such as the Ar Rub'al Khali south of Saudi Arabia (around 52° E and 22° N) or El Djouf in Mauritania (around 10° W and 20° N), show rather low PR backscatter at 0°, for low PR backscatter at 18° (see Figs. 6 and 9). These regions are flat and covered by sand dunes and shifting sands, as described by the FAO. Volume scattering in the dry sand decreases the backscattering. This is easier to observe at 0° incidence angle, where the backscattering over a flat surface should be high.

For low PR backscatters at 18°, the PR backscatters at 0° can show a large range of variations, with two distinct behaviors, one with rather high values and the other with low values. This is confirmed by the histograms (Fig. 10) of the PR backscatter at 0° for PR backscatter at 18° lower than −12 dB, which show two peaks, the left one for dominant volume scattering and the right one with limited volume scattering.

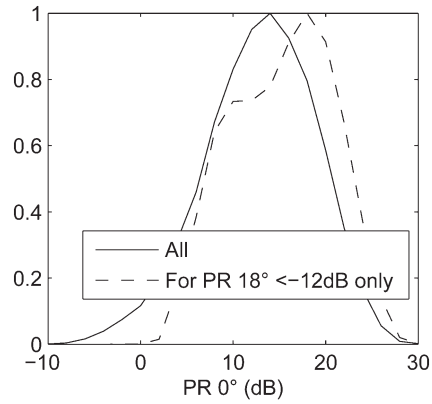

Fig. 10. Normalized histogram of the PR backscattering (in decibels) at 0° over North Africa, for July, for all data, and for PR backscatter at 18° less than −10 dB.

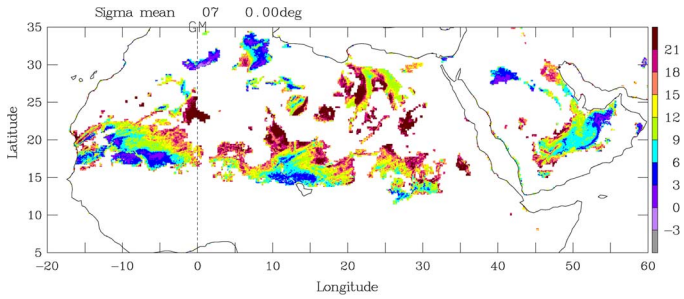

Fig. 11. PR backscattering at 0° (in decibels) when QuikSCAT backscattering (in decibels) at 54° is lower than −18 dB, over the North African desert for July.

CFOSAT will be equipped with two active microwave instruments, one with low observing angles between 0° and 10° and the other one with incidence angles up to 50°. To illustrate the complementarity of the two instruments for the analysis of arid surfaces, Fig. 11 shows the PR backscattering at 0° only for the regions with QuikSCAT backscattering at 54° below −18 dB. A very large variability is observed at 0°. All these regions have low backscattering at 54° because they are flat and/or because they generate high volume scattering. The information provided by the nadir observations helps diagnose the dominant effect. The areas where the backscattering at 0° is also very low correspond to very dry sand, where volume scattering is important (below 20° N and between 10° W and 5° W for instance). On the contrary, the areas where the backscattering at 0° is high are flat regions with very limited volume scattering, i.e., regions that are likely to produce less mineral dust (the region around 23° N and 0° for instance).

The aeolian aerodynamic roughness lengths are the heights above a surface at which the wind profile is assumed to be zero. They are derived from measurements of the wind profile. In arid regions, it has already been estimated from scatterometer data [9], [10], based on spatially coincident satellite observations and *in situ* estimates. The same *in situ* measurements, derived from wind profiles and from geomorphologic analyses, are used here to assess the potential of the satellite Ku observations at different incidence angles to estimate the roughness lengths (see [10] for a detailed description of the *in situ* measurements). Fig. 12 presents the satellite backscattering for different incidence angles (for July), as a function of the *in situ* aerodynamic

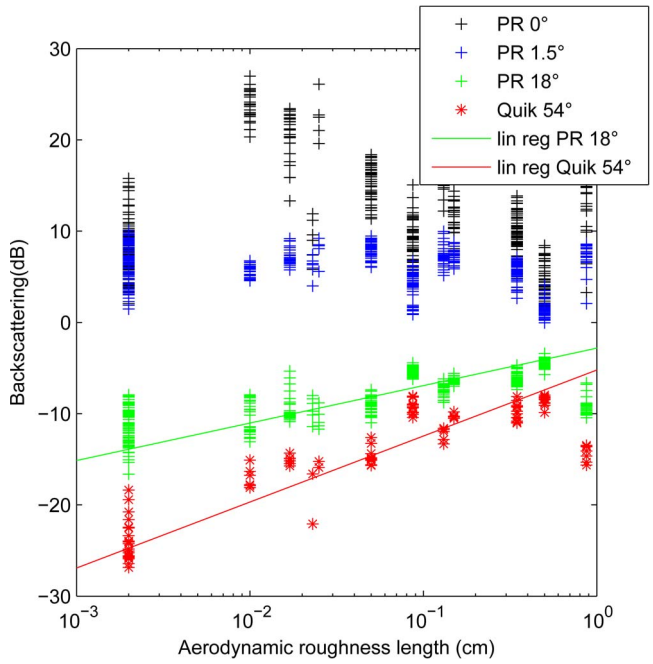

Fig. 12. Backscattering (in decibels) from the PR at 0°, 1.5°, and 18° and from QuikSCAT at 54°, as a function of *in situ* estimate of aerodynamic roughness length (in centimeters) for specific locations in arid regions (log scale). The log linear relationships between the variables are added for PR at 18° and QuikSCAT at 54°.

roughness length (logarithmic scale). For large incidence angles (PR at 18° or QuikSCAT at 54°), the backscattering clearly increases with increasing roughness length. The log linear relationships have been calculated, and they explain respectively 57% and 78% of the variance of the backscattering for PR at 18° and QuikSCAT at 54°. These regressions could be used to estimate the roughness length from the backscattering at these incidence angles. However, at low incidence angles, no relationship can be established between the backscattering and the roughness length. The signal variability is not dominated by this factor.

V. Conclusion

Backscattering in Ku-band (13 GHz) over continental surfaces has been examined, with the TRMM/PR instruments (incidence angles from 0° to 18°), along with observations from the TP altimeter and the QuikSCAT scatterometer (incidence angles around 50°). The signals from the three instruments are very consistent, with the responses at 0° from PR and TP being very close and the responses from QuikSCAT at ∼50° and from PR at 18° being compatible with the changes in incidence angles. The backscattering tends to decrease with increasing vegetation density, as expected, making it possible to classify vegetation density with active microwaves. Over the northern African desert, a very large spatial variability of the backscattering is observed, which is not easy to relate to surface characteristics. Both surface and volume scatterings contribute to the observed signals. With high incidence angle only, it is not possible to discriminate the two effects that have similar signatures (low backscattering). Observations at nadir (0° incidence angle) make it possible to separate the two effects. The use of multiangle observations does help characterize the desert types, but in some areas, the ambiguity of the signals is not yet resolved. The CFOSAT mission will carry two active microwave instruments with a large range of incidence angles, from 0° to 50°. Previous studies have shown the interest of the backscattering with incidence angles above ∼20° for the characterization of arid surfaces. Information has been obtained on the aerodynamic roughness length in arid regions, with significant impact on the aerosol modeling [9], [33]. Our study shows that the combined use of observations at low and high incidence angles adds information on the desert types. Large loads of mineral aerosols from deserts regularly affect the atmosphere in China. With the PR, the largest deserts in China could not be explored, due to the limit of the tropical coverage. The CFOSAT mission will contribute to the monitoring of the sand deserts in Asia, for a better understanding of the mineral aerosol effects and the prediction of the sandstorms.

Note that this study can also contribute to the interpretation of planetary observations, such as the measurements in both active and passive modes obtained from the Cassini mission over Titan, Saturn's largest satellite, where sand deserts have also been detected with microwave observations [34].

Acknowledgment

The authors would like to thank R. Meneghini and W. Olson from NASA for providing them with the TRMM PR surface backscattering archive. Discussion with D. Hauser, a Chinese–French Oceanic SATellite Principal Investigator from the Laboratoire Atmosphères, Milieux, Observations Spatiales, and with J. Munchack from the National Aeronautics and Space Administration was appreciated. The authors would also like to thank three anonymous reviewers for their careful reading of the manuscript and their interesting suggestions.

References

[1] W. Wagner *et al.*, "Evaluation of the agreement between remotely sensed soil moisture data with model and precipitation data," *J. Geophys. Res.*, vol. 108, p. D19, Oct. 2003.

[2] J. Kolassa *et al.*, "Soil moisture retrieval from multi-instrument observations: Part I—Information content analysis and retrieval methodology," *J. Geophys. Res.*, vol. 118, no. 10, pp. 4847–4859, May 2013.

[3] P. J. Harding and M. W. Jackson, "Investigation SeaWinds terrestrial backscatter: Equatorial savannas of South America," *Photogramm. Eng. Remote Sens.*, vol. 69, no. 11, pp. 1243–1245, Nov. 2003.

[4] V. Wismann, K. Boehnke, and C. Schmullius, "Global land surface monitoring using the ERS-1 scatterometer," in *Proc. IGARSS*, 1994, vol. 3, pp. 1488–1490.

[5] P.-L. Frison and E. Mougin, "Use of ERS-1 wind scatterometer data over land surfaces," *IEEE Trans. Geosci. Remote Sens.*, vol. 34, no. 2, pp. 550–560, Mar. 1996.

[6] R. D. Magagi and Y. H. Kerr, "Retrieval of soil moisture and vegetation characteristics by use of ERS-1 wind scatterometer over arid and semi-arid areas," *J. Hydrol.*, vol. 188/189, pp. 361–384, Feb. 1997.

[7] G. Macelloni, S. Paloscia, P. Pampaloni, and E. Santi, "Global scale monitoring of soil and vegetation using SSM/I and ERS wind scatterometer," *Int. J. Remote Sens.*, vol. 24, no. 12, pp. 2409–2425, 2003.

[8] C. Prigent, F. Aires, W. B. Rossow, and E. Matthews, "Joint characterization of vegetation by satellite observations from visible to microwave wavelength: A sensitivity analysis," *J. Geophys. Res.*, vol. 106, no. D18, pp. 20 665–20 685, Sep. 2001.

[9] C. Prigent, I. Tegen, F. Aires, B. Marticorena, and M. Zribi, "Estimation of the aerodynamic roughness length in arid and semi-arid regions over the globe with ERS scatterometer," *J. Geophys. Res.*, vol. 110, no. D9, pp. D09205-1–D09205-12, May 2005.

[10] C. Prigent, C. Jimenez, and J. Catherinot, "Comparison of satellite microwave backscattering (ASCAT) and visible/near-infrared reflectances (PARASOL) for the estimation of aeolian aerodynamic roughness length in arid and semi-arid regions," *Atmos. Meas. Tech.*, vol. 5, no. 2, pp. 2703–2712, Mar. 2012.
[11] K.-H. Lee and E. N. Anagnostou, "A combined passive/ active microwave remote sensing approach for surface variable retrieval using Tropical Rainfall Measuring Mission observations," *Remote Sens. Environ.*, vol. 92, no. 1, pp. 112–125, Jul. 2004.
[12] R. Meneghini *et al.*, "Use of the surface reference technique for path attenuation estimates from the TRMM Precipitation Radar," *J. Appl. Meteorol.*, vol. 39, no. 12, pp. 2053–2070, Dec. 2000.
[13] S. Seto and T. Iguchi, "Rainfall-induced changes in actual surface backscattering cross sections and effects on rain-rate estimates by spaceborne Precipitation Radar," *J. Atmos. Ocean. Technol.*, vol. 24, no. 10, p. 193, 2007.
[14] F. Papa, B. Legresy, and F. Remy, "Use of the Topex–Poseidon dual-frequency radar altimeter over land surfaces," *Remote Sens. Environ.*, vol. 40, pp. 2162–2169, 2003.
[15] F. Papa, C. Prigent, W. B. Rossow, B. Legresy, and F. Remy, "Inundated wetland dynamics over boreal regions from remote sensing: The use of Topex–Poseidon dual-frequency radar altimeter observations," *Int. J. Remote Sens.*, vol. 27, no. 21, pp. 4847–4866, Jan. 2006.
[16] B. Legresy *et al.*, "ENVISAT radar altimeter measurements over continents and ice caps using the Ice-2 retracking algorithm," *Remote Sens. Environ.*, vol. 95, no. 2, pp. 150–163, Mar. 2005.
[17] C. Kummerow, W. Barnes, T. Kozu, J. Shiue, and J. Simpson, "The Tropical Rainfall Measuring Mission (TRMM) sensor package," *J. Atmos. Ocean Tech.*, vol. 15, pp. 808–816, 1998.
[18] W.-T. Tsai, M. Spencer, C. Wu, C. Winn, and K. Kellogg, "SeaWinds on QuikSCAT: Sensor description and mission overview," in *Proc. IEEE IGARSS*, Honolulu, HI, USA, Jul. 24–28, 2000, pp. 1021–1023.
[19] I. Mladenova, V. Lakshmi, J. P. Walker, D. G. Long, and R. De Jeu, "An assessment of QuikSCAT Ku-band scatterometer data for soil moisture sensitivity," *IEEE Geosci. Remote Sens. Lett.*, vol. 6, no. 4, pp. 640–643, Oct. 2009.
[20] L. B. Kunz and D. G. Long, "Calibrating SeaWinds and QuikSCAT scatterometers using natural land targets," *IEEE Geosci. Remote Sens. Lett.*, vol. 2, no. 2, pp. 182–186, Apr. 2005.
[21] S. Frolking, M. Fahnestock, T. Milliman, K. McDonald, and J. Kimball, "Interannual variability in North American grassland biomass/productivity detected by SeaWinds scatterometer backscatter," *Geophys. Res. Lett.*, vol. 32, no. 21, pp. L21409-1–L21409-5, Nov. 2005.
[22] L.-L. Fu *et al.*, "TOPEX/POSEIDON mission overview," *J. Geophys. Res.*, vol. 99, no. C12, pp. 24 369–24 381, Dec. 1994.
[23] *AVISO User Handbook: Merged Topex–Poseidon Products*, CNES, Toulouse, France, Jul. 1996, AVI-NT-02-101-CN (3rd ed.).
[24] H. Stephen and D. G. Long, "Microwave backscatter modeling of erg surfaces in the Sahara desert," *IEEE Trans. Geosci. Remote Sens.*, vol. 43, no. 2, pp. 238–247, Feb. 2005.
[25] Z. Bartalis, K. Scipal, and W. Wagner, "Azimuthal anisotropy of scatterometer measurements over land," *IEEE Trans. Geosci. Remote Sens.*, vol. 44, no. 8, pp. 2083–2092, Aug. 2006.
[26] D. G. Long and M. R. Drinkwater, "Azimuth variation in microwave scatterometer and radiometer data over Antarctica," *IEEE Trans. Geosci. Remote Sens.*, vol. 38, no. 4, pp. 1857–1870, Jul. 2000.
[27] E. Matthews, "Global vegetation and land use: New high-resolution data bases for climate studies," *J. Clim. Appl. Meteorol.*, vol. 22, pp. 474–487, 1983.
[28] T. Kohonen, *Self-Organization and Associative Memory*. New York, NY, USA: Spinger-Verlag, 1984.
[29] Land and Water Development Division, FAO, FAO Food and Agricultural Organization: The Digital Soil Map of the World, 1:5M Scale, Rome 2003.
[30] J. Ridley, F. Strawbridge, R. Card, and H. Phillips, "Radar backscatter characteristics of a desert surface," *Remote Sens. Environ.*, vol. 57, no. 2, pp. 63–78, Aug. 1996.
[31] S. M. S. Bramer, P. A. M. Berry, and J. Carter, "The use of radar altimetry in soil moisture monitoring in support of the SMOS mission," presented at the Earth Observation and Water Cycle Science, Frascati, Italy, 2009, ESA SP-674.
[32] C. Fatras, F. Frappart, E. Mougin, M. Grippa, and P. Hiernaux, "Estimating surface soil moisture over Sahel using ENVISAT radar altimetry," *Remote Sens. Environ.*, vol. 123, pp. 496–507, Aug. 2012.
[33] L. Menut *et al.*, "Impact of surface roughness and soil texture on mineral dust emission fluxes modeling," *J. Geophys. Res.*, vol. 118, no. 12, pp. 6505–6520, Jun. 2013.
[34] R. D. Lorenz *et al.*, "The sand seas of Titan: Cassini RADAR observations of longitudinal dunes," *Science*, vol. 312, no. 5774, pp. 724–727, May 2006.

Catherine Prigent received the Ph.D. degree in physics from the University of Paris, Paris, France, in 1988.

Since 1990, she has been a Researcher for the Centre National de la Recherche Scientifique (CNRS) with the Observatoire de Paris, Paris. From 1995 to 2000, she was on leave from the CNRS, and she worked at the Goddard Institute for Space Studies, National Aeronautics and Space Administration, Columbia University, New York, NY, USA. She is the Cofounder of Estellus, a start-up specialized in satellite Earth observations, and she is also an Adjunct Research Scientist with the Water Center, Columbia University. Her research covers satellite microwave remote sensing of the Earth, for both surface and atmosphere characterizations for global applications. Her early work focused on modeling of the sea surface emissivities at microwave wavelengths and the estimation of atmospheric parameters over ocean from microwave measurements. Key surface parameters include microwave land emissivities, "all weather" determination of land skin temperature, and the first estimates of the wetland extent and dynamics at global scale. She is also involved in satellite remote sensing of clouds with the analysis of passive microwave and millimeter observations over convective cloud structures. Her current main interests concentrate on the atmospheric and surface parameters over land from microwave observations using the synergy with satellite measurements at other wavelength ranges.

Filipe Aires received the Ph.D. degree in statistics from the University of Paris, Dauphine, France, in 1999.

He was an Associate Research Scientist with the Goddard Institute for Space Studies, National Aeronautics and Space Administration (NASA), New York, NY, USA, for five years. He is currently a Research Scientist with the "Laboratoire de Météorologie Dynamique," Centre National de la Recherche Scientifique, Paris, France, and an Adjunct Research Scientist with the Water Center, Columbia University, New York, NY, USA. He is currently on leave at Estellus, Paris, an Institut Pierre-Simon Laplace/Observatoire de Paris spin-off specialized in Earth observation. In earlier works, he analyzed climatic variability using sophisticated mode decomposition, neural networks, or feedback analysis tools. He has developed multi-instrument and multiparameter remote sensing algorithms to retrieve atmospheric variables such as temperature or water vapor profiles, and surface variables such as surface skin temperature, wetland, soil moisture, or infrared/microwave emissivities. The instruments involved in these remote sensing studies include the Advanced Microwave Sounder Unit, Special Sensor Microwave/Imager, Infrared Atmospheric Sounding Interferometer, European Remote-Sensing Satellite, and TIROS Operational Vertical Sounder. He is currently or was a Principal Investigator for NASA, National Oceanic and Atmospheric Administration, European Space Agency, or Centre National d'Etudes Spatiales projects. He was part of the Science and Algorithm Committee of the French–Indian mission Megha-Tropiques in charge of the atmospheric water vapor retrieval chain. He is currently in the science committees of the Surface Water and Ocean Topography and the Global Precipitation Measurement missions and involved in climate impacts in socioeconomic activities. His research interests focus on satellite remote sensing of the Earth and statistical analysis of the climate.

Carlos Jimenez received the Ph.D. degree in environmental science from Chalmers University of Technology, Göteborg, Sweden, in 2003.

From 2007 to 2013, he was a Researcher with the Laboratoire d'Etudes du Rayonnement et de la Matière en Astrophysique, Observatoire de Paris, Paris, France. He is currently with Estellus, Paris. His early work focused on the inversion of satellite limb sounding microwave observations to determine the chemical composition of the Earth's atmosphere. His current main research is related to the analysis of multisatellite observations to characterize different land surface components of the Earth water and energy cycles. He is also involved in satellite remote sensing of ice clouds from analysis of passive microwave observations and is active in the development of submillimeter instruments for future cloud satellite missions.

Fabrice Papa was born in Martigues, France, in 1976. He received the Ph.D. degree from the Centre National d'Etudes Spatiales, Paris, France, and Université Paul Sabatier, Toulouse, France, in 2003.

From 2003 to 2010, he was with the Observatoire de Paris; Goddard Institute for Space Studies, National Aeronautics and Space Administration, Columbia University, New York, NY, USA; and Cooperative Remote Sensing Science and Technology Center, National Oceanic and Atmospheric Administration, City College of New York, New York, NY, USA. Since 2010, he has been with the Laboratoire d'Etudes en Géophysique et Océanographie Spatiales, Institut de Recherche pour le Developpement (IRD), Toulouse, and is currently on deputation at the Indo–French Cell for Water Sciences, IRD–Indian Institute of Science (IISc) Joint International Laboratory, IISc, Bangalore, India. He is particularly focused on the use of multisatellite remote sensing observations to study continental hydrology and its interactions with the ocean and the atmosphere. He is currently a Member of science teams and projects studying the intertropical zone with a special emphasis on the Indian subcontinent and South American regions. His research interests include Earth's observation techniques devoted to study the global water cycle and climate.

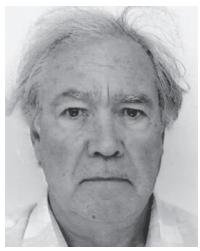

Jack Roger received the degree from the University of Paris-Sud, Orsay, France.

In 1976, he joined the Bureau de Recherche Géologique et Minière (BRGM), Orléans, France. He has been involved in many geological mapping projects in the Middle East (Saudi Arabia and Oman), focusing on the stratigraphic and sedimentologic aspects of Mesozoic and Cenozoic units. Later, since 2000, he has conducted mapping projects in North and West Africa (Morocco, Mali, Mauritania, and Senegal) centered on the stratigraphic aspects of Neoproterozoic and Paleozoic. In 2011, he retired from BRGM.